Effects of temozolomide (TMZ) on the expression and interaction of heat shock proteins (HSPs) and DNA repair proteins in human malignant glioma cells

Gisela Natalia Castro, Niubys Cayado-Gutiérrez, Felipe Carlos Martín Zoppino, Mariel Andrea Fanelli, Fernando Darío Cuello-Carrión

Cell Stress and Chaperones
A Comprehensive Journal of Stress Biology and Medicine

ISSN 1355-8145

Cell Stress and Chaperones
DOI 10.1007/s12192-014-0537-0

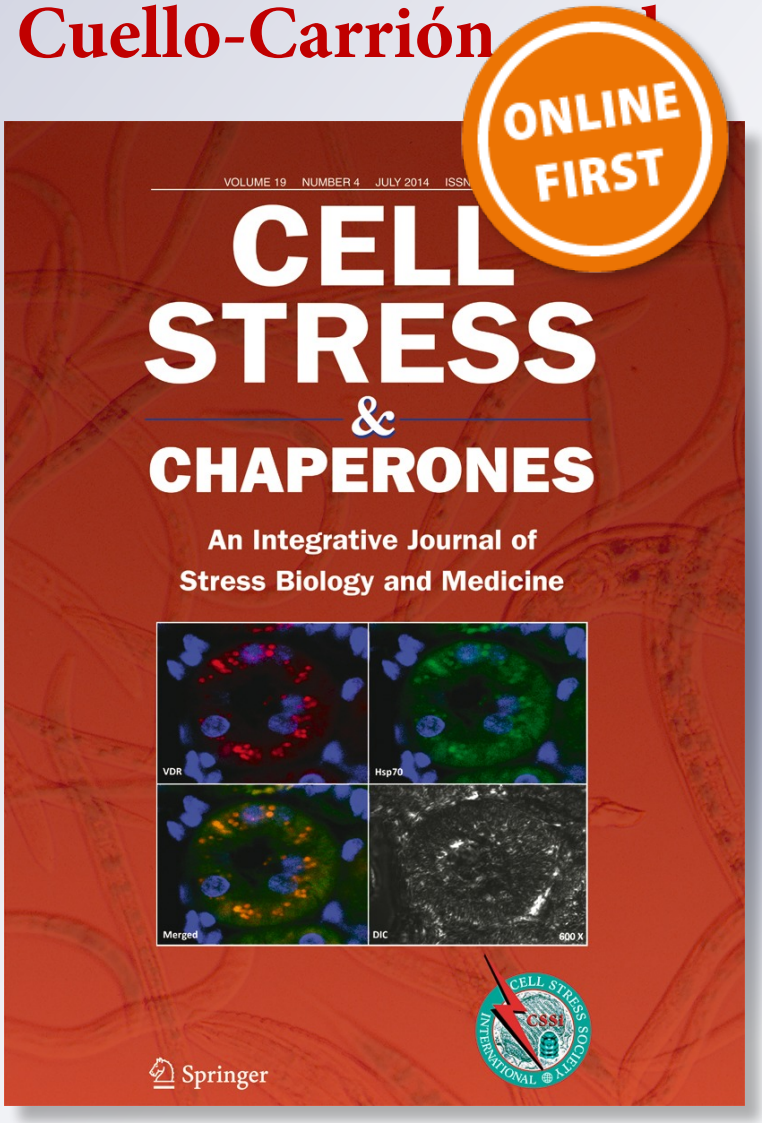

Springer

Cell Stress and Chaperones
DOI 10.1007/s12192-014-0537-0

ORIGINAL PAPER

Effects of temozolomide (TMZ) on the expression and interaction of heat shock proteins (HSPs) and DNA repair proteins in human malignant glioma cells

Gisela Natalia Castro · Niubys Cayado-Gutiérrez · Felipe Carlos Martín Zoppino · Mariel Andrea Fanelli · Fernando Darío Cuello-Carrión · Mayra Sottile · Silvina Beatriz Nadin · Daniel Ramón Ciocca

Received: 20 May 2014 / Revised: 30 July 2014 / Accepted: 10 August 2014

Abstract We previously reported the association of HSPA1A and HSPB1 with high-grade astrocytomas, suggesting that these proteins might be involved in disease outcome and response to treatment. With the aim to better understand the resistance/susceptibility processes associated to temozolomide (TMZ) treatment, the current study was performed in three human malignant glioma cell lines by focusing on several levels: (a) apoptotic index and senescence, (b) DNA damage, and (c) interaction of HSPB1 with players of the DNA damage response. Three human glioma cell lines, Gli36, U87, and DBTRG, were treated with TMZ evaluating cell viability and survival, apoptosis, senescence, and comets (comet assay). The expression of HSPA (HSPA1A and HSPA8), HSPB1, O_6-methylguanine-DNA methyltransferase (MGMT), MLH1, and MSH2 was determined by immunocytochemistry, immunofluorescence, and Western blot. Immunoprecipitation was used to analyze protein interaction. The cell lines exhibited differences in viability, apoptosis, and senescence after TMZ administration. We then focused on Gli36 cells (relatively unstudied) which showed very low recovery capacity following TMZ treatment, and this was related to high DNA damage levels; however, the cells maintained their viability. In these cells, MGMT, MSH2, HSPA, and HSPB1 levels increased significantly after TMZ administration. In addition, MSH2 and HSPB1 proteins appeared co-localized by confocal microscopy. This co-localization increased after TMZ treatment, and in immunoprecipitation analysis, MSH2 and HSPB1 appeared interacting. In contrast, HSPB1 did not interact with MGMT. We show in glioma cells the biological effects of TMZ and how this drug affects the expression levels of heat shock proteins (HSPs), MGMT, MSH2, and MLH1. In Gli36 cells, the results suggest that interactions between HSPB1 and MSH2, including co-nuclear localization, may be important in determining cell sensitivity to TMZ.

Keywords Temozolomide · Glioma · HSPB1 · MSH2 · MGMT

Introduction

Temozolomide (TMZ) is the main drug administrated to patients suffering from high-grade gliomas. These tumors are highly invasive and lethal due to the development of resistance to therapies. Although many therapeutic approaches have been explored, there has been no major improvement in survival over the last years. The epigenetic inactivation (promoter methylation) status of the DNA repair enzyme O_6-methylguanine-DNA methyltransferase (MGMT) is used to guide this treatment (Park et al. 2013; Stupp et al. 2007; Thomas et al. 2013). However, since tumor cells have many mechanisms to deal with drug treatment, the characterization of other molecular mechanisms that might be implicated in the resistance to anticancer treatment is needed as a step toward more individualized treatment concepts. For example,

Castro, Cayado-Gutiérrez, Nadin, and Ciocca contributed equally to this work.

G. N. Castro · N. Cayado-Gutiérrez · F. C. M. Zoppino · M. A. Fanelli · F. D. Cuello-Carrión · D. R. Ciocca (✉)
Oncology Laboratory, IMBECU-CCT, CONICET, National Research Council, Av. Dr. Ruiz Leal s/n, Parque General San Martín, CP 5500 Mendoza, Argentina
e-mail: dciocca@mendoza-conicet.gob.ar

M. Sottile · S. B. Nadin
Tumor Biology Laboratory, IMBECU-CCT, CONICET, National Research Council, Av. Dr. Ruiz Leal s/n, Parque General San Martín, CP 5500 Mendoza, Argentina

Published online: 26 August 2014

aldehyde dehydrogenase (ALDH) 1A1 is under investigation as predictor of TMZ resistance (Schäfer et al. 2012). On the other hand, suppression of hypoxia-inducible factor 1α (HIF-1α) has been shown to sensitize glioblastoma cells to TMZ treatment via down-modulation of MGMT expression (Chen et al. 2013).

In a previous study in human gliomas, we reported that heat shock proteins (HSPs) HSPB1 and HSPA together with β-catenin, P53, and MGMT were associated with high-grade astrocytomas, suggesting that these markers are associated with the disease outcome and the response to treatments (Castro et al. 2012). In addition, in oligodendroglial tumors, HSPB1 appeared as a surrogate molecular marker of loss of heterozygosity (LOH) of 1p (Castro et al. 2012). HSPB1 is overexpressed in high-grade gliomas and involved in disease prognosis (Castro et al. 2012; Ciocca and Calderwood 2005). HSPB1 is implicated in drug resistance through several molecular mechanisms described elsewhere (Ciocca et al. 2013). In a recent study, the inhibition of the HSP response increased the antitumor activity of PS-341 (bortezomib, Velcade), a highly specific 26S proteasome inhibitor, increasing the cell death of two glioblastoma cell lines (Liu et al. 2012). HSPB1 can enter the nucleus and apparently although it is not capable of repairing DNA damage independently, it can efficiently contribute to DNA repair as part of their molecular chaperone function (Nadin and Ciocca 2010).

The mismatch repair (MMR) system is one of the DNA repair mechanisms that contribute to both the maintenance of the genome integrity/stability and the prevention of carcinogenesis (Fishel et al. 1993). MMR components, i.e., MLH1 and MSH2, recognize and correct DNA mismatches as protein heterodimers. The MMR system and the MGMT enzyme are responsible for repairing the DNA damages induced by TMZ, and it has been determined that cells that have a deficient MMR system and high expression levels of MGMT may be resistant to treatment (Omar and Mason 2010). Nadin et al. (2007) reported in peripheral blood lymphocytes from healthy subjects exposed in vitro to hyperthermia and cisplatin that MLH1 and MSH2 (MMR proteins) co-localize with HSPB1 and HSPA. Hyperthermia induced the nuclear accumulation of HSPB1 and affected the subcellular localization of MLH1 and MSH2 in human colon cancer cells (Nadin et al. 2012). In patients with gliomas, deficiency of DNA MMR proteins seems to contribute to glioblastoma progression since in recurrent tumors, MLH1 expression was found significantly reduced (Stark et al. 2010). This is consistent with another study where a low expression of MSH2, MSH6, and PMS2 (MMR proteins) in patients with glioblastomas correlated with disease recurrence after the standard treatment (Felsberg et al. 2011). In addition, these authors reported that *MGMT* promoter methylation (but not MGMT protein expression) was associated with longer progression-free survival, overall survival, and post-recurrence survival, but no changes in *MGMT* promoter methylation were noted in recurrent glioblastomas.

While TMZ has a significant impact on the survival of high-grade glioma patients, tumor recurrence and drug resistance remain major challenges. Moreover, TMZ treatment can cause several toxicities to the patients (Marosi 2012). Therefore, we are attempting to find new molecular markers to predict tumor response to TMZ and to search additional molecular targets to improve glioma therapy. For this purpose, we studied the biological effect of TMZ administration in three glioma cell lines analyzing the expression levels of proteins related to treatment resistance and DNA repair: HSPA (HSPA8 and HSPA1A), HSPB1, MGMT, MLH1, and MSH2.

Materials and methods

Cell lines and treatment

Three human malignant glioma cell lines were used: Gli36, a kind gift from Dr. Carlos Palacios (Institute of Science and Technology, Dr. Cesar Milstein, Buenos Aires), and U87-MG (U87) and DBTRG 0.5 MG (DBTRG), kindly donated by Dr. Martin Radrizzani (National University of General San Martín, Buenos Aires). The cells were originally acquired from American Type Culture Collection (ATCC). Cells were grown in complete Dulbecco's modified Eagle medium (DMEM) (GIBCO) and Roswell Park Memorial Institute (RPMI) (Sigma-Aldrich), supplemented with 10 % fetal bovine serum (GIBCO) in a culture oven with 5 % CO_2. The cells were subjected to TMZ administration at concentrations which ranged between 0 and 500 μM for 24 h in order to simulate that the drug levels reached in the clinical practice (single daily treatment of TMZ at 75 mg/m^2) (Brandes et al. 2009). In most experiments, we used TMZ concentrations (0–25 μM) equivalent to drug doses achieved in cerebral spinal fluid (CSF) of patients after treatment (Patel et al. 2003; Ostermann et al. 2004). The drug was obtained from LKM Laboratories, and it was dissolved in dimethyl sulfoxide (DMSO, Sigma). The final concentration of DMSO in the culture medium did not exceed 0.01 %, which did not influence the cell viability and the expression of the proteins under study.

Cytotoxicity assays

Viability (dose–response curves)

In the 3-(4,5-dimethylthiazol-2-yl)-2,5-diphenyltetrazolium bromide (MMT) assay, the cells were washed with culture medium free of serum, and 2 mL phosphate-buffered saline (PBS) containing 1 mg/mL MTT (Sigma-Aldrich) was added

to each well. The medium was discarded after 4 h, DMSO was added to dissolve MTT-formazan derivative, and formazan was quantified by measuring absorbance at 550 nm wavelength as described previously (Liu et al. 1997).

Clonogenic assay

Cells (500) were seeded in a six-well plate. After 24 h, cells received TMZ treatment and the cells were allowed to grow and recover for 10–14 days to form colonies. The colonies were fixed with cold methanol and stained with Crystal violet (0.5 %). The viable colonies containing more than 50 cells were counted and the surviving fraction was calculated.

Immunocytochemistry

Cells (80,000) were seeded on glass coverslips and exposed to the different TMZ concentrations. After washing, the cells were fixed in formol 4 % in PBS 1× (prepared for dilution 1:10 of PBS 10×, 1.4 M NaCl; 0.03 M KCl; 0.1 M Na_2PO_4H; 0.2 M KPO_4H_2). Fixed cells were permeabilized with 0.5 % (*v*/*v*) Triton X-100 for 5 min and incubated with rabbit polyclonal antibody against a hybrid Hsp27/Hsp25 protein (1:1,000, kindly provided by Dr. Gaestel, Germany), mouse monoclonal HSPB1 (1:500 Stressgen Biotech, Corp., Victoria, Canada), and mouse monoclonal HSPA (clone BMR22, 1:1,000, Sigma-Aldrich, USA); the BRM22 clone detects both HSPA1A and HSPA8 proteins, mouse monoclonal MGMT (clone MT23.2, 1:50 Zymed, USA), mouse monoclonal MSH2 (1:500 Merck Millipore, USA), mouse monoclonal MLH1 (1:1,000, Becton Dickinson, Pharmingen), and mouse monoclonal P53 (DO7, 1:50, Dako, Carpinteria, CA). The antigen retrieval protocol with heat was used to unmask the antigens (30 min in citrate buffer 0.01 M, pH 6.0). Slides were lightly counterstained with hematoxylin to reveal nuclei, and they were observed and photographed with a Nikon Eclipse E200 microscope (×60 objective). Nonspecific mouse IgG1 antibody and purified rabbit pre-immune serum (DAKO, Kingsgrove, NSW, Australia) were used as isotype negative controls.

Apoptosis analysis

Apoptosis was assessed by the modification of the terminal deoxynucleotidyl transferase-mediated dUTP nick end-labeling (TUNEL) assay using the ApopTag Plus in situ detection kit (Millipore, Temecula, CA); according to previously reported (Cuello-Carrion and Ciocca 1999). The apoptotic index (AI) was calculated as the percentage of positive nuclei, based on an average of 200 cells, at ×400 magnification.

Senescence-associated β-galactosidase assay

Fifty thousand cells were seeded in a six-well plate on sterile coverslip. Then, the cells were treated with different concentrations of TMZ for 24 h. SA-β-Gal staining was performed as previously described (Dimri et al. 1995). Briefly, cells were fixed with 2 % formaldehyde and 0.2 % glutaraldehyde for 5 min and incubated overnight at 37 °C with 1 mg/mL X-gal staining solution (5-bromo-4-chloro-3-indolyl β-D-galactoside, 5 mM $K_3Fe[CN]_6$, 5 mM $K_4Fe[CN]_6$, and 2 mM $MgCl_2$ in PBS, pH 6.0). The cells were rinsed twice with PBS, washed with methanol, and examined using a Nikon Eclipse E200 microscope (Nikon Corp., Tokyo, Japan).

Alkaline comet assay

This method was performed according to the procedure previously described (Olive et al. 1992). To prevent additional DNA damage, the assay was done in the dark and at 4 °C. After electrophoresis, the agarose gels were silver stained (Nadin et al. 2001). Comets were evaluated in duplicate samples and under double blindness, using the ×20 objective of a Nikon optic microscope, counting 40 randomly selected cells per slide (that is, 80 cells/each sample). A visual score based on extend of migration was used: 0, very low migration; 1, 5–10 % of migrated DNA; 2, 11–30 % of migrated DNA; 3, 31–60 % of migrated DNA; 4, 61–95 % of migrated DNA; and 5, >95 % of migrated DNA (Anderson et al. 1994). To facilitate the management of the data, an average of DNA migration was calculated as [(% of cells with score 1)× 1+(% of cells with score 2)*x*2+(% of cells with score 3)×3+ (% of cells with score 4)×4+(% of cells with score 5)×5]/100 (Branham et al. 2004). As a positive control, we used cells treated with 60 μM of hydrogen peroxide for 1 h.

Immunofluorescence (confocal microscopy)

Tumor cells were fixed with 2 % paraformaldehyde in PBS for 10 min at 37 °C, washed with PBS, and blocked with 50 mM NH_4Cl in PBS. Cells were permeabilized with 0.05 % saponin in PBS containing 0.5 % BSA and incubated with primary antibody against Hsp25/27 (1:50) and mouse monoclonal antibody against MSH2 (1:50). After washing, cells were incubated with secondary antibody conjugated with Alexa Fluor 555 (Invitrogen, 1:500) and Alexa Fluor 488 (Invitrogen, 1:500). Gli36 cells were mounted with Mowiol (Sigma-Aldrich, Argentina) and examined by confocal microscopy using FV1000 Olympus confocal microscope and FV10-ASW 1.7 software (Olympus, Japan). Appropriate negative controls were included. Analysis of images was performed using the software ImageJ (Wayne Rasband, National Institutes of Health). Briefly, median intensity of green and red channels was determined in randomly selected

areas with similar size [region of interest (ROI)] localized at the nuclear zone, at least 200 cells were analyzed per experiment. A threshold value was established according to visual analysis [median fluorescence intensity (MFI): 500]. Above and below of MFI value, the cells were classified as positive or negative to MSH2 nuclear expression, respectively, then HSPB1 nuclear expression was evaluated in the same manner. ROI regions were organized and evaluated using the ROI Manager tool. Data were presented as intensity mean values.

Immunoprecipitation (IP) and Western blotting (WB)

IP analyses were performed using monoclonal antibodies against HSPB1 (12 μg), MSH2 (10 μg), and MGMT (12 μg). They were covalently coupled to M-280 tosyl-activated Dynabeads (Invitrogen Dynal AS, Oslo, Norway) according to the manufacturer's protocol. Total lysates (1,000 μg of proteins) from untreated and TMZ-treated Gli36 cells were subjected to IP with HSPB1, MSH2, and MGMT (control)-coated beads, respectively, for 1 h with tilting and rotation. After washing with PBS, the beads were resuspended in sample buffer, and the target protein bound was eluted and concentrated by boiling for 5 min at 97 °C. WB analyses of supernatants (before and after spinning down the immune complex) were performed using 20 μg of total protein.

Western blot assay was performed as previously described (Fanelli et al. 2008). Cell supernatants with 50 μg of total proteins were loaded on 12 % sodium dodecyl sulfate polyacrylamide gel (SDS-PAGE). The antibodies used were rabbit antibody against Hsp25/27 (1:200), mouse antibody against MSH2 (1:400), mouse antibody against MGMT (1:50), mouse monoclonal BRM22 clone against HSPA (HSPA8 and HSPA1A) (1:1,000), and mouse monoclonal MLH1 (1:500). The immunoblot images were capture using LAS-4000 imaging system (Fujifilm Life Science, USA) and evaluated using NIH image V1.62 program (NIH, Bethesda, MD, USA).

Statistical analysis

Statistical studies were assessed by column analyses with one-way ANOVA with Bonferroni's and Dunnett's posttests and Student's *t* test. The level of significance was set at $p<0.05$. The data were analyzed using the Prism computer program (GraphPad Software, San Diego, CA).

Results

The viability of the three cells lines was relatively high when the cells were exposed to TMZ, for example at 25 μM, which is the approximate concentration attainable by the drug in the CSF (Patel et al. 2003; Ostermann et al. 2004). Gli36 cells showed 95 % viability, while DBTRG and U87 cells showed 80 % viability approximately (Fig. 1). The IC50 for the cells was far beyond the therapeutic concentrations (Gli36 160 μM, DBTRG 90 μM, U87 330 μM). Apoptosis evaluated by the TUNEL technique was significantly different in the three cells lines, but apoptotic indexes were relatively low, not exceeding 13 %. Significant differences in the induction of apoptosis by TMZ treatment were observed only in DBTRG cells (Fig. 1). Figure 2a shows TUNEL examples in Gli36 cells before and after TMZ treatment.

The senescence levels were quite different in the three cell lines. Senescence was not observed in Gli36 cells, U87 had very low levels that were not significant modified by TMZ treatment, while DBRTG cells reached relatively high levels (Fig. 1).

Gli36 showed very low recovery capacity by clonogenic assay to TMZ-induced damage, and this was related to the high DNA damage shown in the comet assay (Fig. 3). Whereas DBTRG line exhibited an intermediated recovery capacity associated to a lower. In DNA damage at 25 μM TMZ treatment, U87 cells showed the most long-term survival related to intermediate DNA damage, resulting to be least sensitive to TMZ treatment. We then were interested in DNA repair systems in these cell lines, Gli36 in particular, since they showed low capacity to form colonies but retained their viability.

In Western blot studies, Gli36 cells showed low MGMT levels in untreated conditions, but the enzyme increased significantly when TMZ was administered. In contrast, in DBRTG cells, MGMT levels decreased following TMZ administration while U87 cells displayed no significant depletion in MGMT levels (Fig. 4). The expression levels of MLH1 and MSH2 are shown in Fig. 4. These proteins were expressed in untreated cells. DBTRG cells showed the highest MLH1 and MSH2 levels after TMZ administration. A significant increase in MSH2 protein was found in Gli36 cell line. Immunocytochemical studies support these results; MLH1 and MSH2 proteins appeared mainly in the nuclei of cell lines analyzed (Fig. 5).

In addition, HSPB1 and HSPA expression was determined by WB (Fig. 6). These HSPs were constitutively expressed in the three untreated cell lines. In particular, Gli36 cells showed the lowest HSPB1 basal levels. However, HSPB1 expression increased after TMZ treatment in the three cell lines, and significant changes in HSPA were seen in Gli36 and DBTRG cells. Furthermore, HSPB1 was seen in the nuclei (by immunocytochemistry) mainly in Gli36 after drug administration, but this expression was not uniform in all cells; there were cell clusters that displayed the protein in the cytoplasmic region around the nucleus (Fig. 6b).

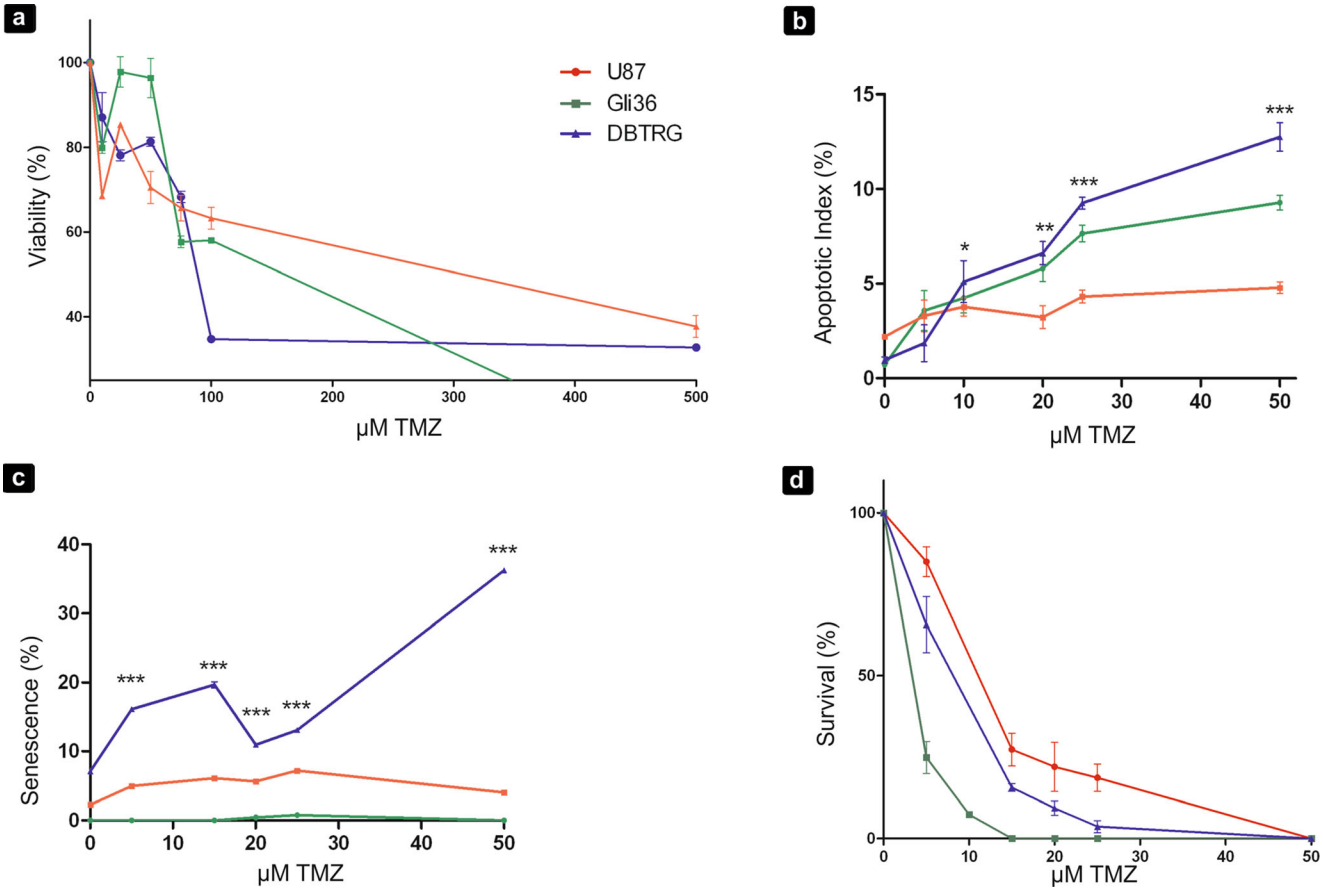

Fig. 1 Biological effects of TMZ in glioma cells. High percentages of viability were noted in the three cell lines even at elevated TMZ concentrations (**a**). The induction of apoptosis was relatively low in all three cell lines, and significant differences were observed only in DBTRG cells (**b**). Senescence showed a significant increase only in the DBTR cells while Gli36 cells did not show senescence (**c**). Survival: Gli36 showed the lowest recovery capacity to the damage induced by TMZ, while U87 cells were the relatively insensitive to treatment (**d**). Analysis of variance (ANOVA) and Dunnett's test were performed. Results are the mean± standard deviations (SD) of three independent experiments. *Error bars* represent standard error of the mean (SEM). *Asterisks* (*) indicate *p*-values<0.05

On the basis of these results, considering the particular biological behavior observed in Gli36 and since little is known on this line (Han et al. 2013; Verreault et al. 2013), we focused our studies in these cells. Surprisingly, a nuclear co-localization between HSPB1 and MSH2 was observed before and after TMZ treatment in a minor subpopulation of Gli36 cells when they were examined by confocal microscopy (Fig. 7a). It is noteworthy that only nuclear positive MSH2 cells showed a significant increase of nuclear HSPB1 expression after TMZ treatment (Fig. 7b). Meanwhile, a low nuclear HSPB1 expression was determined in nuclear negative MSH2 cells, and it did not significantly change with the treatment. We also observed a substantial cytoplasmic co-localization of both proteins, which was not analyzed in this work due to our interest in the role played by MSH2 and HSPB1 proteins in the nucleus.

We next examined by immunoprecipitation if MSH2 and HSPB1 were interacting in Gli36 cells (Fig. 7c). This study demonstrated that HSPB1 and MSH2 interact in a higher proportion after administration of TMZ. HSPB1 expression was not detected by WB before and after IP because only 20 μg of total proteins was loaded and the amount of HSPB1 in the original homogenate was very low, as we mentioned above. We also analyzed the existence of a possible HSPB1 and MGMT protein interaction but we did not find it (negative control).

Discussion

In recent years, TMZ has become the treatment of choice for malignant gliomas and, although the molecular mechanism of action of this drug is known (Dolan and Pegg 1997), important details remain to be elucidated. This is the first study that reports the expression profile of HSPs simultaneously with DNA repair proteins after TMZ administration in human glioma cells. The three glioma cell lines showed significant differences in TMZ-induced toxicity, and we emphasize here the elevated cell viability found at therapeutic concentrations. At 25 μM of TMZ, DBTRG cells were the most sensitive to

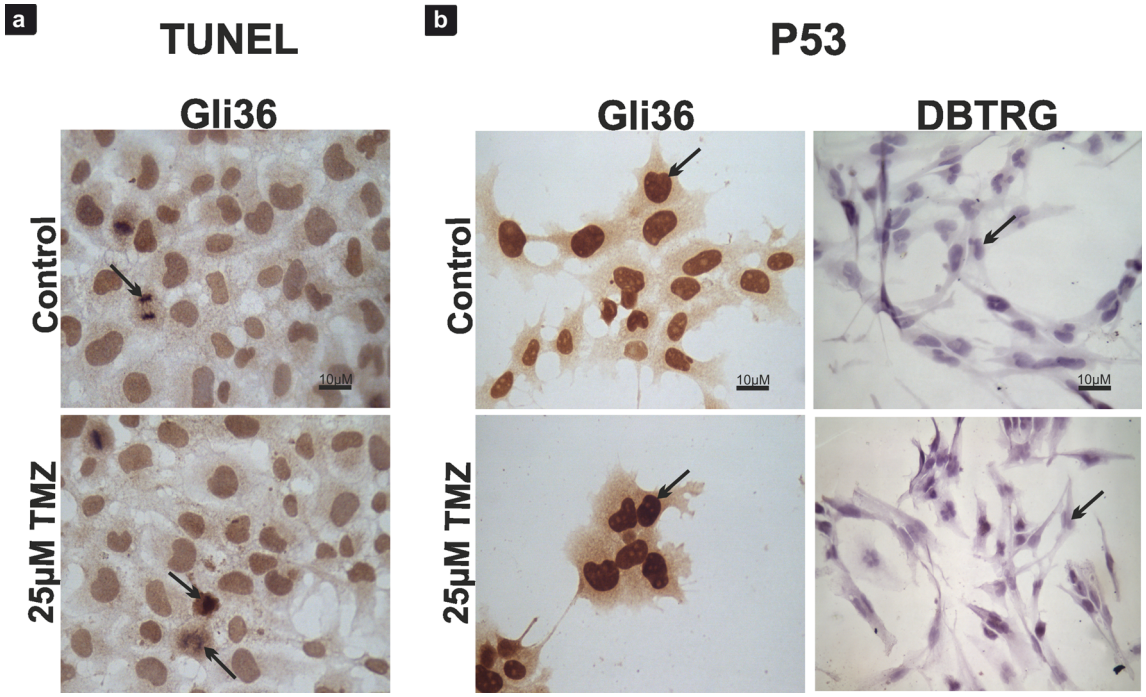

Fig. 2 Apoptosis and P53 status in glioma cells. Representative images of apoptosis by TUNEL assay before and after TMZ treatment in Gli36 cells (**a**). *Arrows* highlight mitotic cells and apoptotic figure in TMZ-treated cells. Note the low TMZ-induced apoptosis. Representative immunocytochemical staining of P53 in Gli36 and DBTRG cells (**b**). *Arrows* indicate positive immunoreactivity that appears as brown deposits (mutant or inactive P53) in Gli36 cells. In DBTRG cells, *arrows* show negative immunoreaction (P53-wt). The slides were lightly counterstained with hematoxylin

the drug treatment, and they still showed a cell viability of 77 %. The presence of HSPA and MGMT proteins in glioma cells has been associated with cell progression and resistance to therapy (Li et al. 2011; Liu et al. 2011; Nager et al. 2012); therefore, the decreased expression of these proteins found in our study could explain the higher sensitivity to the drug in DBTRG cells. In contrast, Gli36 cells presented the lowest percentage of sensitivity at 25 μM of TMZ, which was associated with high levels of HSPA and MGMT supporting that these proteins could be conferring resistance to TMZ. At the same drug concentration, U87 showed no pronounced cytotoxic effects and almost no increase in HSPA expression; the other studied proteins did not show changes that could be correlated with the biological behavior in this cell line. In agreement with our study, Paolini et al. (2011) reported no changes in HSPA levels before and after TMZ treatment even when they used higher doses (200 μM) in U87 cell line; in addition, there were no cytotoxic effects.

In the last years, promising agents for primary brain tumors in vitro have had little impact on the disease outcome in clinical trials. The lack of success in the results may be at least partly explained by the inability to deliver therapeutic agents to the CNS tumors across the blood–brain barrier (Laquintana et al. 2009). Drug delivery to the brain is hampered by the presence of P-glycoprotein (P-gp, ABCB1), breast cancer resistance protein (BCRP, ABCG2), and multidrug resistance-associated proteins (MRPs, ABCC1) (Veringa et al. 2013). In glioma cell lines, MDR1 P-glycoprotein and ABCC1 were shown to confer resistance to various anticancer drugs (Spiegl-Kreinecker et al. 2002; Bronger et al. 2005). Finally, there are other molecular mechanisms that contribute to chemoresistance such as upregulation of antiapoptotic pathways, enhanced DNA repair mechanisms, and increased metabolic inactivation with subsequent removal of the drugs applied (Bronger et al. 2005). Our study was aimed to improve the understanding of mechanisms involved in TMZ resistance; two alternative mechanisms of tumor suppression were studied: apoptosis and senescence. It seems important to mention that the apoptotic indexes were low at TMZ therapeutic concentrations and that each cell line showed a different behavior to treatment. DBTRG exhibited a relatively higher apoptotic index, whereas Gli36 cell line had an intermediate apoptotic index, and TMZ did not induce apoptosis in U87 cells. Our results are consistent with other previously reported (Hirose et al. 2001). The authors studied the role of P53 in TMZ-treated U87 cells demonstrating that P53 wild-type (wt) was present in U87 cells and that few of these cells underwent TMZ-induced apoptosis. On the other hand, DBTRG cells had P53-wt (Morandi et al. 2008), and these cells showed increased apoptotic cell death. Due to the lack of previous data, we evaluated P53 status in Gli36 cell line, and we found nuclear P53 overexpression before and

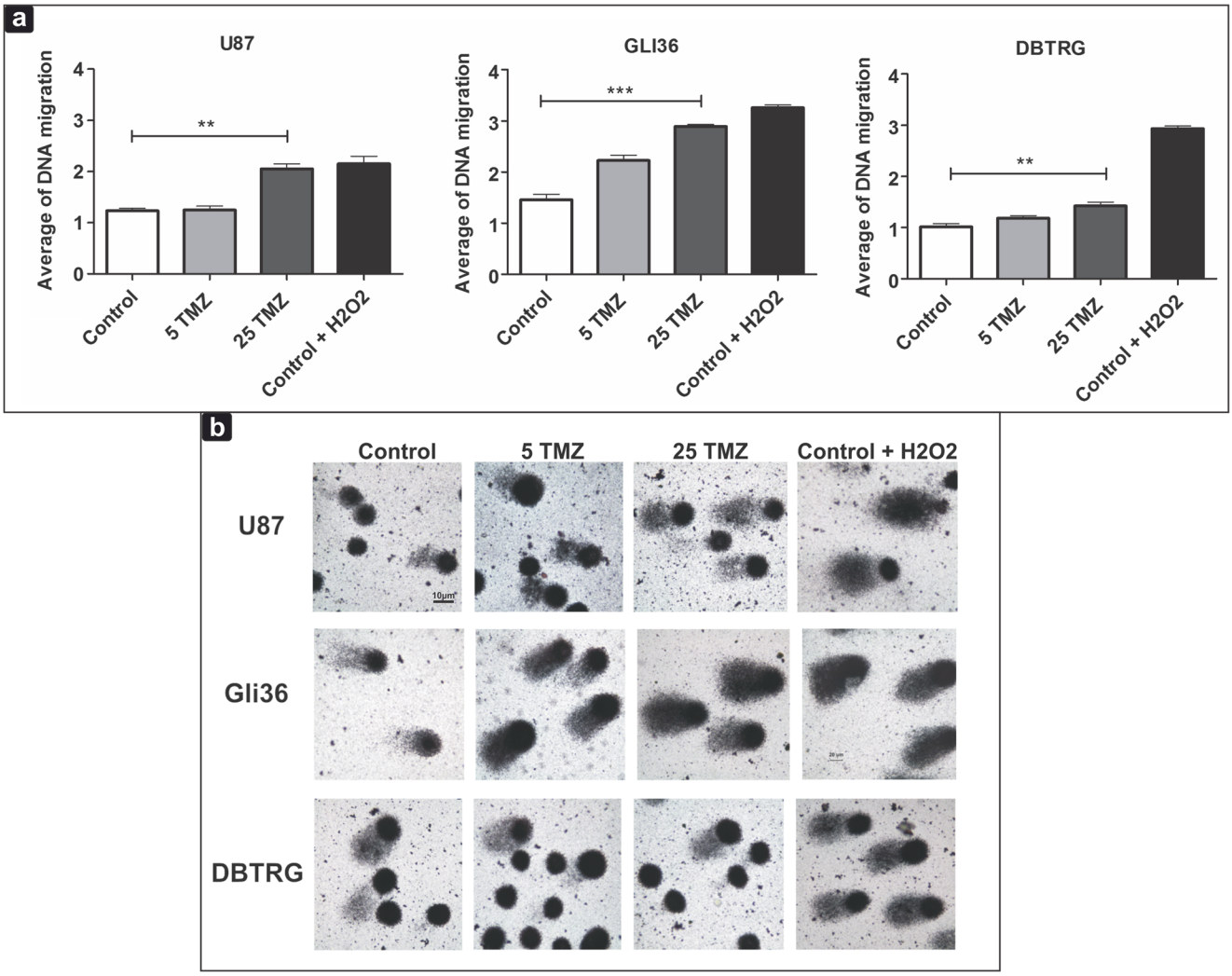

Fig. 3 DNA damage induced by TMZ in glioma cell lines. Bars graphs (**a**) and representative photographs (**b**) of comet assay for U87, Gli36, and DBTRG cells. Gli36 cells exhibited the highest DNA damage, while the lower damage was observed in DBTRG cells. Statistical analysis was performed using one-way ANOVA and Dunnett's posttest. Results are the mean±standard deviations (SD) of three independent experiments; *error bars* represent standard error of the mean (SEM). *Asterisks* (*) indicate p values<0.05

after TMZ demonstrating the presence of the mutant or inactive protein form [mutant P53 forms stable complexes with proteins reaching a long half-life and accumulates within the nucleus (Nagao et al. 1995; Mitsumoto et al. 2004)] (Fig. 2b). These results suggest that in Gli36 cells, TMZ may induce apoptosis by a P53-independent mechanism and that apoptosis could not be related to MGMT (Sato et al. 2009) or to HSPA expression levels. Further studies are needed to address the molecular players involved in apoptosis of gliomas to allow a better correlation with the results obtained in the present work.

On the other hand, senescence was observed solely in the cell lines with functional P53-wt (DBTRG and U87). Then, we focused our study on DBTRG and Gli36 cells because they showed high or lack of senescence, respectively. HSPB1 and HSPA expression levels were examined in these cell lines. Recently, two reports from the same research group demonstrated in various human cancer cell lines (but not in gliomas) that induction of senescence by downregulation of HSPB1 is associated with activation of the P53 pathway and with the induction of P21 (O'Callaghan-Sunol et al. 2007; Yaglom et al. 2007), then HSPB1 seems to play a role in regulation of cellular senescence by modulating the P53 pathway. They also found that HSPA1A protein provided a selective advantage to cancer cells by suppressing default senescence via P53-dependent and P53-independent pathways (O'Callaghan-Sunol et al. 2007; Yaglom et al. 2007). Our study showed that TMZ-treated DBTRG cells had a significant decrease in HSPA expression which leads to an increase of senescence, suggesting that reduced expression of HSPA sensitizes this cell line to TMZ treatment. In contrast to these authors, TMZ treatment increased HSPB1 and senescence

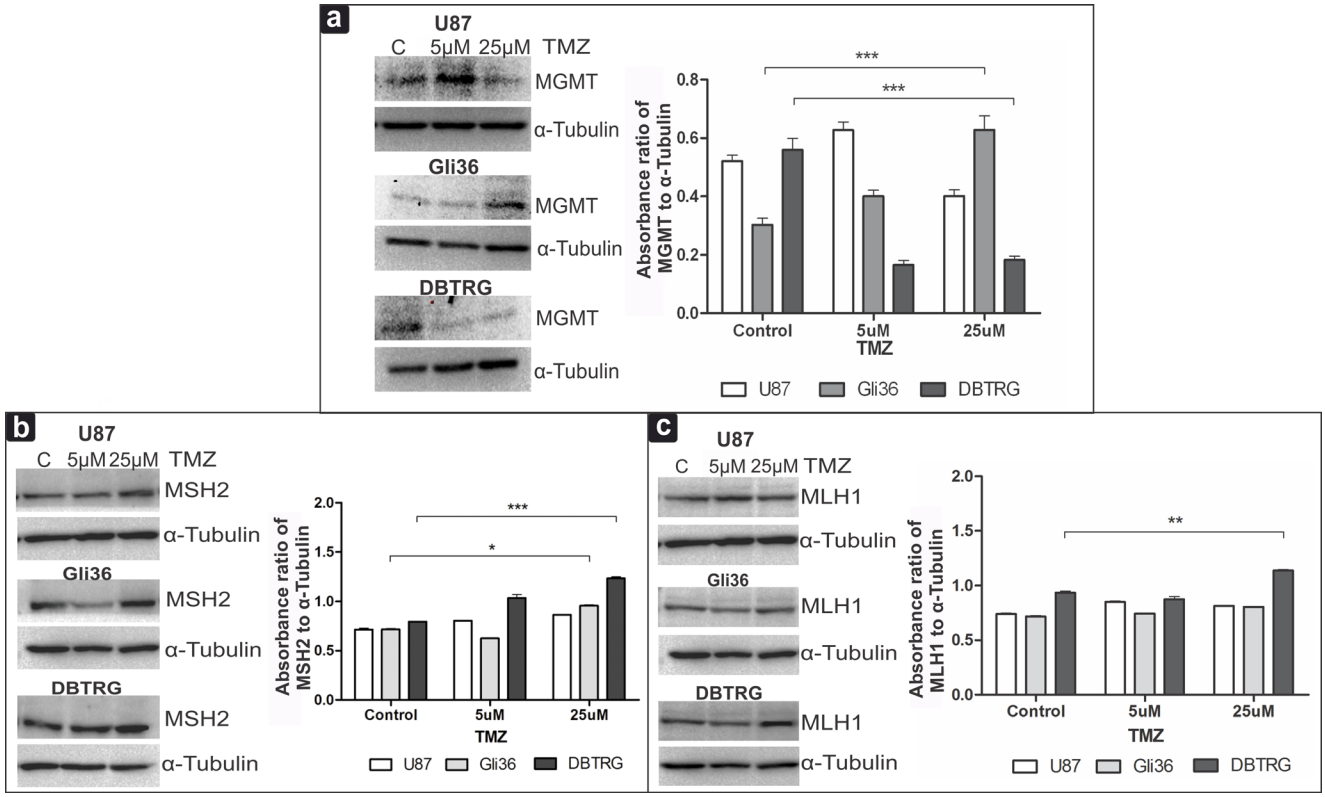

Fig. 4 TMZ effects on MGMT, MSH2, and MLH1 expression. Representative immunoblots of MGMT (**a**), MSH2 (**b**), and MLH1 (**c**) in U87, Gli36, and DBTRG cells. Gli36 cells showed significant increase in MGMT and MSH2 levels after treatment. DBTRG cells showed the highest MLH1 and MSH2 expression after TMZ. Immunoblot evaluation was performed using NIH image V1.62 program. *Bars* represent absorbance ratio of studied proteins to α-tubulin. Statistical analysis was performed using one-way ANOVA and Dunnett's posttest. Data shown are means±standard errors of three independent experiments. The level of significance was set at $p<0.05$

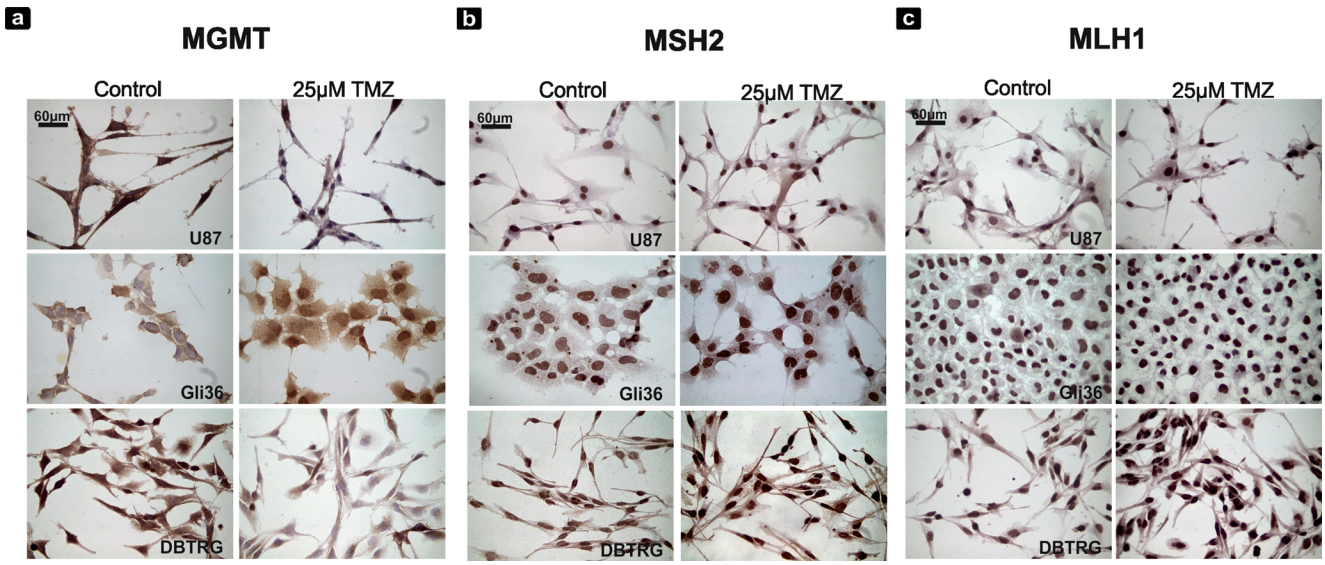

Fig. 5 Immunocytochemical staining to reveal MGMT, MSH2, and MLH1 proteins in glioma cells. Representative images of MGMT (**a**), MSH2 (**b**), and MLH1 (**c**) expression in U87, Gli36, and DBTRG cells before and after TMZ treatment. Gli36 cells showed low MGMT levels in control and a significant increase after treatment. In DBRTG cells, MGMT levels decreased with TMZ administration, while U87 cells displayed no significant depletion. MSH2 and MLH1 proteins were located mainly in the nuclei of the three cell lines. Positive immunoreactivity appears as brown deposits, and the slides were lightly counterstained with hematoxylin

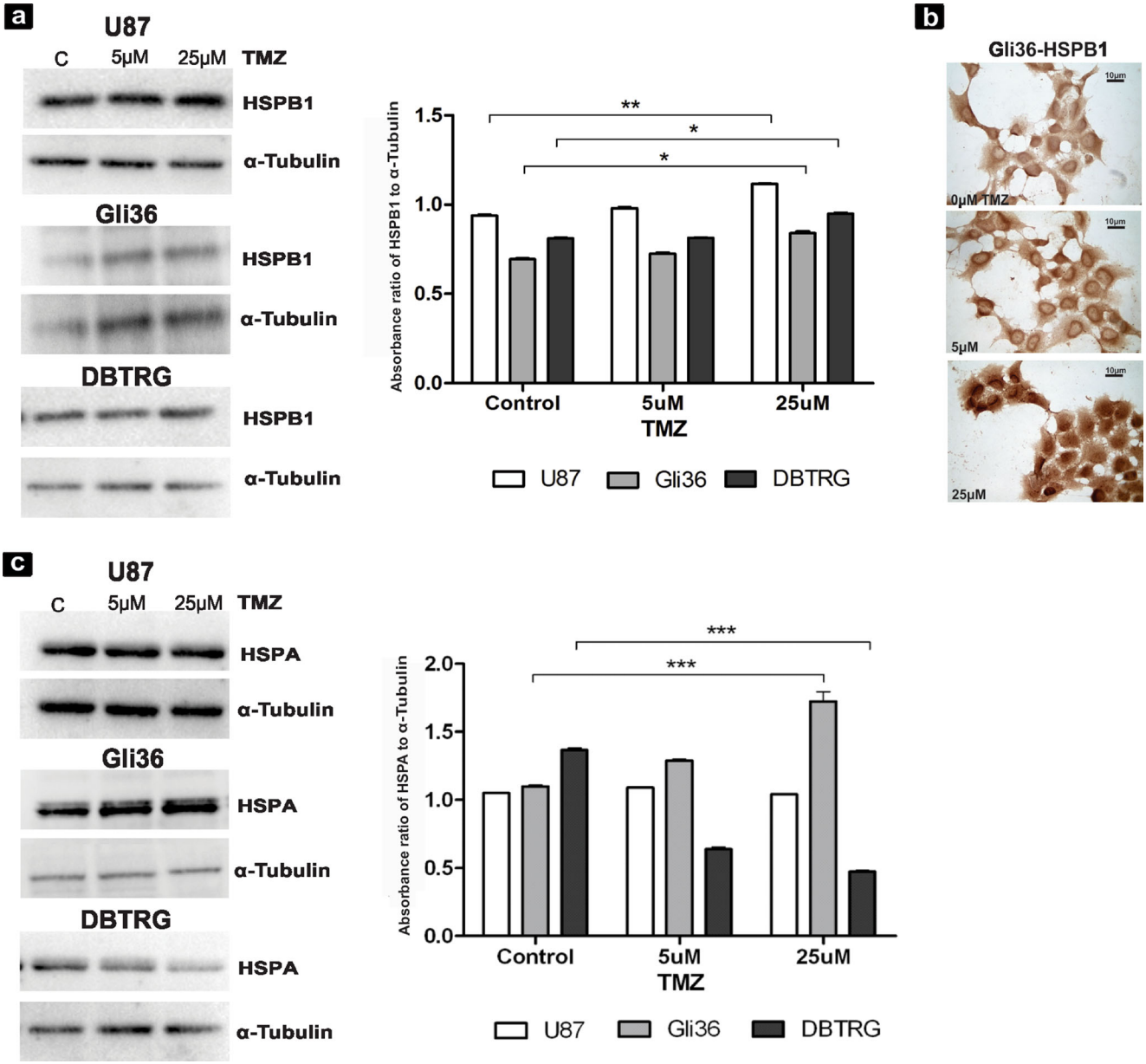

Fig. 6 TMZ effects on HSPB1 and HSPA expression. Representative immunoblots of HSPB1 in U87, Gli36, and DBTRG cell lines (**a**). *Bars* represent absorbance ratio of HSPB1 to α-tubulin. High levels of HSPB1 were seen after treatment in the three cell lines. Immunocytochemical images showing HSPB1 expression in Gli36 cell line (**b**). Note the localization change from cytoplasm to nucleus of HSPB1 after TMZ treatment. Positive immunoreactivity appears as brown deposits, and the slides were lightly counterstained with hematoxylin. HSPA expression in U87, Gli36, and DBTRG cell lines (**c**). *Bars* represent that absorbance ratio of HSPA to α-tubulin significant changes in HSPA was seen in Gli36 and DBTRG cells. Data show means±standard errors calculated from three independent experiments. *Asterisk* (*) indicates significant change of protein expression using one-way ANOVA and Dunnett's posttest

levels were observed, suggesting that in DBTRG cells, the senescence process could be activated by a P53-independent pathway. On the other hand, TMZ increased HSPA and HSPB1 expressions in Gli36 cells. Taking into account that Gli36 cells have an inactive P53 form, we suggest that the senescence process was blocked by P53-independent pathways. These results are in agreement with those previously reported by Yaglom et al. (2007). Further studies will be required to understand the mechanisms of senescence related to HSPA in human gliomas. Currently, the development of HSPA1A inhibitors may become a novel and interesting approach to increase the sensitivity of cancer cells to overcoming resistance to chemotherapy.

Our study contributes to the knowledge on the association of HSPs with TMZ resistance in human glioma cell lines. This is the first report showing that TMZ increases HSPB1 expression in two glioma cell lines (DBTRG and Gli36) and that TMZ affects HSPA expression. In contrast, in another human

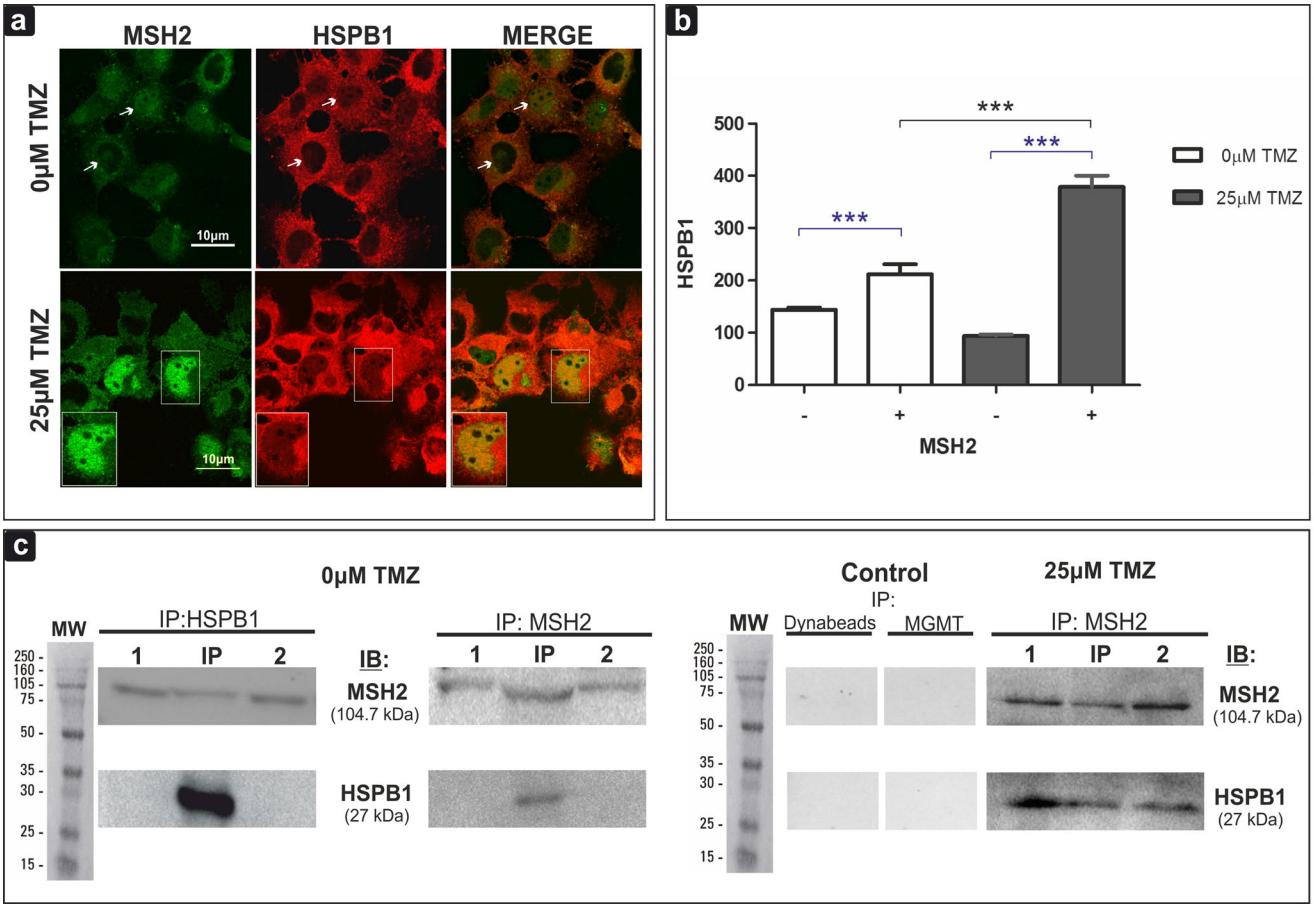

Fig. 7 Co-localization and interaction analyses of HSPB1 and MSH2 in Gli36 cells. Representative fluorescence images of the nuclear co-localization of HSPB1 and MSH2 before and after TMZ treatment (**a**). Before TMZ treatment (control), the *arrows* point to nuclei with and without HSPB1 and MSH2. The *insets* show the co-localization of both proteins in TMZ-treated cells. Graph analysis of mean fluorescence intensity (**b**). Cells were classified according to MSH2 nuclear expression (+/−), and then, the HSPB1 expression was evaluated (see "Materials and methods"). Note the significant increase in the co-localization between MSH2 and HSPB1 after TMZ treatment ($p<0.0001$). Statistical analysis was performed by Student's *t* test; *error bars* indicate the standard error of the mean from at least three independent experiments. Protein interaction between HSPB1 and MSH2 was found by immunoprecipitation studies, and this interaction increased in TMZ-treated cells (25 μM) (**c**). Control IP using: Dynabeads (without cell lysate) and mouse monoclonal antibody against MGMT. *MW* molecular weight markers (Full Range Rainbow from Amersham, GE Healthcare, UK). *1* Gli36 cell supernatant (total lysate 20 μg/μL) before IP. *2* same as 1 but after IP

glioma cell line (MOGGCCM, astrocytoma GIII), a previous study showed an inhibition of HSPB1 and HSPA1A expression after treatment with TMZ, alone or in combination with quercetine (Jakubowicz-Gil et al. 2010). This is indicating that TMZ is inducing different responses in different glioma cells, and the molecular heterogeneity may be important in understanding how current therapeutic treatments fail to target cells in the GBM tumor mass thereby selecting for resistant cells that can result in disease recurrence and poor survival (Chorny et al. 2000). In fact, genomic and proteomic analyses have identified various subtypes of GBM (proneural, mesenchymal, classical, and neural) (Karsy et al. 2012). The present study provides new insights into the complex molecular mechanisms used by glioma cells to resist anticancer treatments.

Long-term survival after TMZ treatment was differentially affected in the three cell lines, and this could be attributed to TMZ-induced DNA damages and the status of the DNA repair systems. TMZ induces O6-methylguanine (O_6-meG) lesions that are repaired by MGMT; if this enzyme is not acting on O_6-meG pairs with thymine during DNA replication, this mispair is recognized by the MMR system leading to a recursive cycling of excision and synthesis which produce DNA strand breaks that activate DNA damage signaling pathways, leading to cell death (York and Modrich 2006). To gain insight into this matter, we have evaluated the DNA damage (comet assay) and the expression of the DNA repair proteins: MGMT, MLH1, and MSH2. High MGMT expression levels coupled to a defective MMR system can mediate resistance to TMZ (Friedman et al. 2000; Omar and Mason 2010). Gli36 cells exhibited the lower long-term survival which correlated with the highest percentage of DNA damage (at 25 μM TMZ). However, this cell line had the lowest cytotoxic effect. This is not very surprising because MGMT expression was increased,

and MLH1 and MSH2 nuclear expressions were observed in response to 25 μM of TMZ suggesting that these proteins could be involved in the particular biological behavior observed in Gli36. DBTRG cells exhibited an intermediate long-term survival, and they presented the lowest DNA damage to 25 μM TMZ treatment. These cells exhibited a favorable molecular profile to treatment response (low MGMT expression and high MLH1 and MSH2 levels) showing drug sensitivity; our results are consistent with previous reports (Friedman et al. 2000; Omar and Mason 2010). On the other hand, U87 cells were the most resistant to TMZ showing a great long-term survival and an intermediate level of DNA damage at 25 μM of TMZ. Moreover, these cells showed high MGMT levels and stable expression levels of MLH1 and MSH2 suggesting other molecular mechanisms of drug resistance.

There is previous evidence that HSPB1 and other small HSPs may carry out functions specifically related to their subcellular localization which is a key parameter dictating and mediating their biological function (Michaud et al. 2008). Previous studies using peripheral blood mononuclear cells demonstrated that nuclear translocation of HSPB1 and HSPA1A after doxorubicin treatment was associated with a high expression of MLH1 and MSH2 (Nadin et al. 2003). Moreover, we have reported that MLH1 and MSH2 co-localize with HSPB1 and HSPA1A in peripheral blood lymphocytes from healthy patients (Nadin et al. 2007). We report here that HSPB1 and MSH2 co-localize in Gli36 cell nuclei in the absence of drug, and this co-localization was significantly increased after TMZ. We noted substantial HSPB1 and MSH2 co-localization in the cytoplasm as well, but at present, we do not have a clear explanation on the functional consequence(s) of the interaction at this level. In addition, we suggest the changes in the nuclear HSPB1 expression could be TMZ-dependent. The immunoprecipitation studies supported the interaction between both proteins, and further studies are necessary to conclude that the interaction between MSH2 and HSPB1 may affect the functionality of the MMR system in glioma cells. Previous reports have demonstrated that HSPs

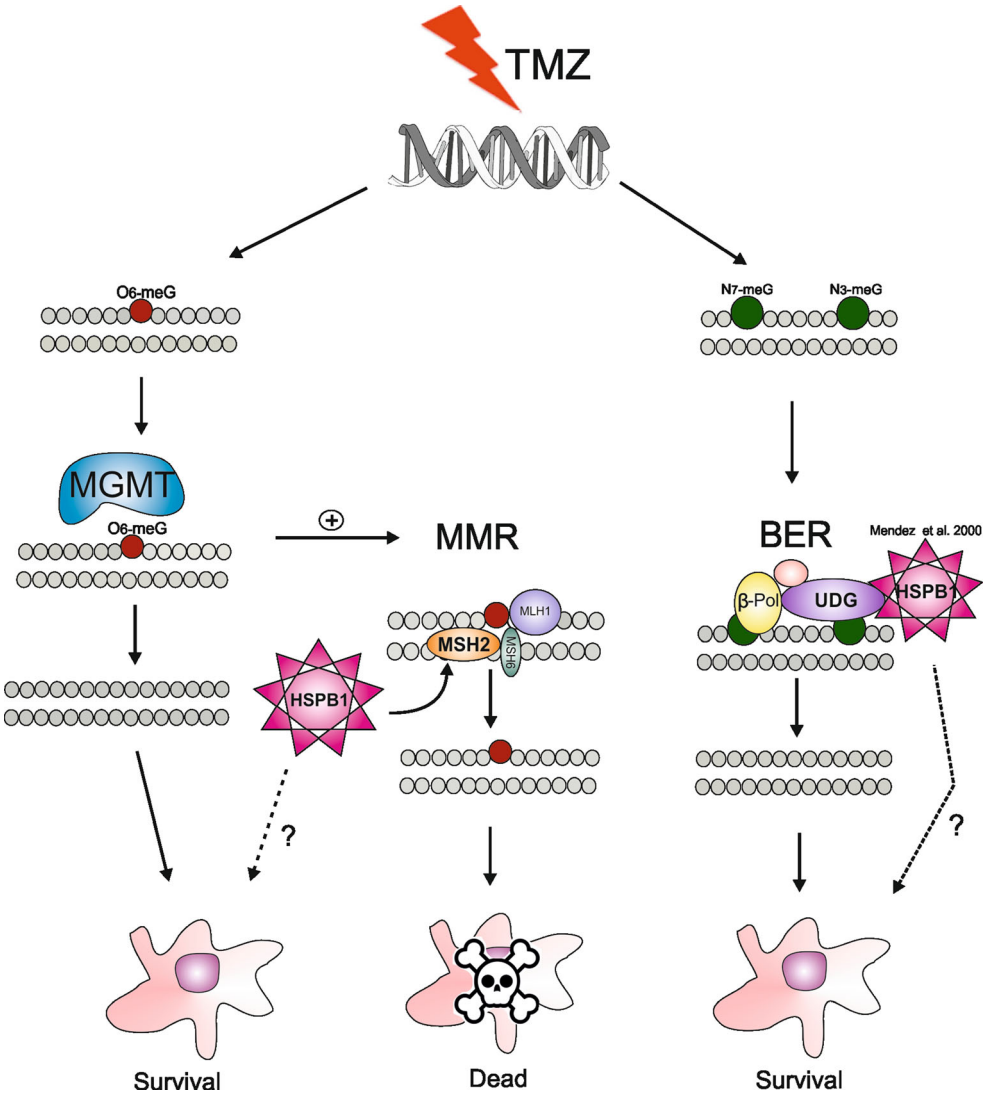

Fig. 8 Proposed role of HSPB1 in the DNA repair systems induced by TMZ in human glioma cells. TMZ causes cytotoxic DNA lesions such as O_6-methylguanine (O_6-meG) and N_7-methylguanine (N_7-meG). MGMT removes the O_6-meG DNA adducts causing cell survival. If the DNA adducts escape the MGMT repair mechanism, mismatched base pairs will appear during DNA replication. These are recognized by the MMR system resulting in futile repair cycles leading to cell death. N_7-meG DNA adducts are efficiently repaired by the base excision repair (BER) pathway, and normally, they contribute little to TMZ cytotoxicity. We propose that the interaction of HSPB1 with MSH2 may affect the functionality of MMR system in human malignant glioma cells contributing to TMZ resistance mechanisms

are involved in DNA repair mechanisms, in human head-and-neck cancer cell lines. Guttmann et al. (2013) found that HSPB1 co-localize with ATM in both untreated and irradiated cells showing a possible involvement of HSPB1 in double strand break repair system. Enzymes of the base excision repair system (uracil DNA glycosylase and AP endonuclease) have also been associated with HSPB1 and HSPA (Mendez et al. 2000). We propose a potential role of HSPB1 in the MMR system and its consequences on TMZ resistance mechanism in human gliomas. This model should be interpreted inside the context of complex mechanisms of drug resistance (Fig. 8). A recent study by Sang et al. (2014) in U87 cells suggests the importance of HSPB1 phosphorylation in the mechanisms of TMZ resistance; we are beginning to study this important subject.

Acknowledgments This study was funded by the National Research Council (CONICET) of Argentina (PIP 2012–2014).

Conflict of interest None declared.

References

Anderson D, Yu TW, Phillips BJ, Schmezer P (1994) The effect of various antioxidants and other modifying agents on oxygen-radical-generated DNA damage in human lymphocytes in the COMET assay. Mutat Res 307:261–271

Brandes A, Franceschi E, Tosoni A, Benevento F, Scopece L, Mazzocchi V, Bacci A, Agati R, Calbucci F, Ermani M (2009) Temozolomide concomitant and adjuvant to radiotherapy in elderly patients with glioblastoma: correlation with MGMT promoter methylation status. Cancer 115:3512–3518

Branham MT, Nadin SB, Vargas-Roig LM, Ciocca DR (2004) DNA damage induced by paclitaxel and DNA repair capability of peripheral blood lymphocytes as evaluated by the alkaline comet assay. Mutat Res 560:11–17

Bronger H, König J, Kopplow K, Steiner HH, Ahmadi R et al (2005) ABCC drug efflux pumps and organic anion uptake transporters in human gliomas and the blood-tumor barrier. Cancer Res 65: 11419–11428

Castro GN, Cayado-Gutiérrez N, Moncalero VL et al (2012) Hsp27 (HSPB1): a possible surrogate molecular marker for loss of heterozygosity (LOH) of chromosome 1p in oligodendrogliomas but not in astrocytomas. Cell Stress Chaperones 17:779–790

Chen W, Xiao Z, Zhao Y, Huang L, Du G (2013) HIF-1alpha inhibition sensitizes pituitary adenoma cells to temozolomide by regulating MGMT expression. Oncol Rep 30:2495–2501

Chorny JA, Evans LC, Kleinschmidt-DeMasters BK (2000) Cerebral granular cell astrocytomas: a Mib-1, bcl-2, and telomerase study. Clin Neuropathol 19:170–179

Ciocca DR, Calderwood SK (2005) Heat shock proteins in cancer: diagnostic, prognostic, predictive, and treatment implications. Cell Stress Chaperones 10:86–103

Ciocca DR, Arrigo AP, Calderwood SK (2013) Heat shock proteins and heat shock factor 1 in carcinogenesis and tumor development: an update. Arch Toxicol 87:19–48

Cuello-Carrion FD, Ciocca DR (1999) Improved detection of apoptotic cells using a modified in situ TUNEL technique. J Histochem Cytochem 47:837–839

Dimri GP, Lee X, Basile G et al (1995) A biomarker that identifies senescent human cells in culture and in aging skin in vivo. Proc Natl Acad Sci U S A 92:9363–9367

Dolan ME, Pegg AE (1997) O6-benzylguanine and its role in chemotherapy. Clin Cancer Res 3:837–847

Fanelli MA, Montt-Guevara M, Diblasi AM et al (2008) P-cadherin and beta-catenin are useful prognostic markers in breast cancer patients; beta-catenin interacts with heat shock protein Hsp27. Cell Stress Chaperones 13:207–220

Felsberg J, Thon N, Eigenbrod S et al (2011) Promoter methylation and expression of MGMT and the DNA mismatch repair genes MLH1, MSH2, MSH6 and PMS2 in paired primary and recurrent glioblastomas. Int J Cancer 129:659–670

Fishel R, Lescoe MK, Rao MR, Copeland NG, Jenkins NA, Garber J, Kane M, Kolodner R (1993) The human mutator gene homolog MSH2 and its association with hereditary nonpolyposis colon cancer. Cell 75:1027–1038

Friedman HS, Kerby T, Calvert H (2000) Temozolomide and treatment of malignant glioma. Clin Cancer Res 6:2585–2597

Guttmann DM, Hart L, Du K, Seletsky A, Koumenis C (2013) Inhibition of Hsp27 radiosensitizes head-and-neck cancer by modulating deoxyribonucleic acid repair. Int J Radiat Oncol Biol Phys 87:168–175

Han C, Zhao R, Kroger J, Qu M, Wani AA, Wang QE (2013) Caspase-2 short isoform interacts with membrane-associated cytoskeleton proteins to inhibit apoptosis. PLoS One 8:e67033

Hirose Y, Berger MS, Pieper RO (2001) p53 effects both the duration of G2/M arrest and the fate of temozolomide-treated human glioblastoma cells. Cancer Res 61:1957–1963

Jakubowicz-Gil J, Langner E, Wertel I, Piersiak T, Rzeski W (2010) Temozolomide, quercetin and cell death in the MOGGCCM astrocytoma cell line. Chem Biol Interact 188:190–203

Karsy M, Gelbman M, Shah P, Balumbu O, Moy F, Arslan E (2012) Established and emerging variants of glioblastoma multiforme: review of morphological and molecular features. Folia Neuropathol 50:301–321

Laquintana V, Trapani A, Denora N, Wang F, Gallo JM, Trapani G (2009) New strategies to deliver anticancer drugs to brain tumors. Expert Opin Drug Deliv 6:1017–1032

Li G, Xu Y, Guan D, Liu Z, Liu DX (2011) HSP70 protein promotes survival of C6 and U87 glioma cells by inhibition of ATF5 degradation. J Biol Chem 286:20251–20259

Liu Y, Peterson DA, Kimura H, Schubert D (1997) Mechanism of cellular 3-(4,5-dimethylthiazol-2-yl)-2,5-diphenyltetrazolium bromide (MTT) reduction. J Neurochem 69:581–593

Liu C, Tu Y, Sun X et al (2011) Wnt/beta-catenin pathway in human glioma: expression pattern and clinical/prognostic correlations. Clin Exp Med 11:105–112

Liu Y, Zheng T, Zhao S et al (2012) Inhibition of heat shock protein response enhances PS-341-mediated glioma cell death. Ann Surg Oncol 19:S421–S429

Marosi C (2012) Complications of chemotherapy in neuro-oncology. Handb Clin Neurol 105:873–885

Mendez F, Sandigursky M, Franklin WA, Kenny MK, Kureekattil R, Bases R (2000) Heat-shock proteins associated with base excision repair enzymes in HeLa cells. Radiat Res 153:186–195

Michaud S, Lavoie S, Guimond MO, Tanguay RM (2008) The nuclear localization of Drosophila Hsp27 is dependent on a monopartite arginine-rich NLS and is uncoupled from its association to nuclear speckles. Biochim Biophys Acta 1783:1200–1210

Mitsumoto Y, Nakajima T, Marutani M, Kashiwazaki H, Moriguchi M, Kimura H, Okanoue T, Kagawa K, Tada M (2004) Loss of p53 transcriptional activity in hepatocellular carcinoma evaluated by yeast-based functional assay: comparison with p53 immunohistochemistry. Hum Pathol 35:350–356

Morandi E, Severini C, Quercioli D et al (2008) Gene expression time-series analysis of camptothecin effects in U87-MG and DBTRG-05 glioblastoma cell lines. Mol Cancer 7:66

Nadin SB, Ciocca DR (2010) Participation of heat shock proteins in DNA repair mechanisms in cancer. In: Thomas AE (ed) DNA damage repair, repair mechanisms and aging, 1st edn. Nova Science Publishers, Inc, New York, pp 165–186

Nadin SB, Vargas-Roig LM, Ciocca DR (2001) A silver staining method for single-cell gel assay. J Histochem Cytochem 49:1183–1186

Nadin SB, Vargas-Roig LM, Cuello-Carrion FD, Ciocca DR (2003) Deoxyribonucleic acid damage induced by doxorubicin in peripheral blood mononuclear cells: possible roles for the stress response and the deoxyribonucleic acid repair process. Cell Stress Chaperones 8:361–372

Nadin SB, Vargas-Roig LM, Drago G, Ibarra J, Ciocca DR (2007) Hsp27, Hsp70 and mismatch repair proteins hMLH1 and hMSH2 expression in peripheral blood lymphocytes from healthy subjects and cancer patients. Cancer Lett 252:131–146

Nadin SB, Cuello-Carrión FD, Sottile ML, Ciocca DR, Vargas-Roig LM (2012) Effects of hyperthermia on Hsp27 (HSPB1), Hsp72 (HSPA1A) and DNA repair proteins hMLH1 and hMSH2 in human colorectal cancer hMLH1-deficient and hMLH1-proficient cell lines. Int J Hyperth 28:191–201

Nagao T, Kondo F, Sato T, Nagato Y, Kondo Y (1995) Immunohistochemical detection of aberrant p53 expression in hepatocellular carcinoma: correlation with cell proliferative activity indices, including mitotic index and MIB-1 immunostaining. Hum Pathol 26:326–333

Nager M, Bhardwaj D, Canti C, Medina L, Nogues P, Herreros J (2012) beta-Catenin signalling in glioblastoma multiforme and glioma-initiating cells. Chemother Res Pract 2012:192362

O'Callaghan-Sunol C, Gabai VL, Sherman MY (2007) Hsp27 modulates p53 signaling and suppresses cellular senescence. Cancer Res 67: 11779–11788

Olive PL, Wlodek D, Durand RE, Banath JP (1992) Factors influencing DNA migration from individual cells subjected to gel electrophoresis. Exp Cell Res 198:259–267

Omar AI, Mason WP (2010) Temozolomide: the evidence for its therapeutic efficacy in malignant astrocytomas. Core Evid 4:93–111

Ostermann S, Csajka C, Buclin T, Leyvraz S, Lejeune F, Decosterd LA, Stupp R (2004) Plasma and cerebrospinal fluid population pharmacokinetics of temozolomide in malignant glioma patients. Clin Cancer Res 10:3728–3736

Paolini A, Pasi F, Facoetti A, Mazzini G, Corbella F, Di Liberto R, Nano R (2011) Cell death forms and HSP70 expression in U87 cells after ionizing radiation and/or chemotherapy. Anticancer Res 31: 3727–3731

Park CK, Lee SH, Kim TM, Choi SH, Park SH, Heo DS, Kim IH, Jung HW (2013) The value of temozolomide in combination with radiotherapy during standard treatment for newly diagnosed glioblastoma. J Neurooncol 112:277–283

Patel M, McCully C, Godwin K, Balis FM (2003) Plasma and cerebrospinal fluid pharmacokinetics of intravenous temozolomide in non-human primates. J Neurooncol 61:203–207

Sang DP, Li RJ, Lan Q (2014) Quercetin sensitizes human glioblastoma cells to temozolomide in vitro via inhibition of Hsp27. Acta Pharmacol Sin 35:832–838

Sato Y, Kurose A, Ogawa A, Ogasawara K, Traganos F, Darzynkiewicz Z, Sawai T (2009) Diversity of DNA damage response of astrocytes and glioblastoma cell lines with various p53 status to treatment with etoposide and temozolomide. Cancer Biol Ther 8:452–457

Schäfer A, Teufel J, Ringel F et al (2012) Aldehyde dehydrogenase 1A1—a new mediator of resistance to temozolomide in glioblastoma. Neuro Oncol 14:1452–1464

Spiegl-Kreinecker S, Buchroithner J, Elbling L et al (2002) Expression and functional activity of the ABC-transporter proteins P-glycoprotein and multidrug-resistance protein 1 in human brain tumor cells and astrocytes. J Neurooncol 57:27–36

Stark AM, Doukas A, Hugo HH, Mehdorn HM (2010) The expression of mismatch repair proteins MLH1, MSH2 and MSH6 correlates with the Ki67 proliferation index and survival in patients with recurrent glioblastoma. Neurol Res 32:816–820

Stupp R, Hegi ME, Gilbert MR, Chakravarti A (2007) Chemoradiotherapy in malignant glioma: standard of care and future directions. J Clin Oncol 25:4127–4136

Thomas RP, Recht L, Nagpal S (2013) Advances in the management of glioblastoma: the role of temozolomide and MGMT testing. Clin Pharmacol 5:1–9

Veringa SJ, Biesmans D, van Vuurden DG, Jansen MH et al (2013) In vitro drug response and efflux transporters associated with drug resistance in pediatric high grade glioma and diffuse intrinsic pontine glioma. PLoS One 8:e61512

Verreault M, Weppler SA, Stegeman A, Warburton C, Strutt D, Masin D, Bally MB (2013) Combined RNAi-mediated suppression of Rictor and EGFR resulted in complete tumor regression in an orthotopic glioblastoma tumor model. PLoS One 8:e59597

Yaglom JA, Gabai VL, Sherman MY (2007) High levels of heat shock protein Hsp72 in cancer cells suppress default senescence pathways. Cancer Res 67:2373–2381

York SJ, Modrich P (2006) Mismatch repair-dependent iterative excision at irreparable O6-methylguanine lesions in human nuclear extracts. J Biol Chem 281:22674–22683